International Journal of Engineering Inventions
e-ISSN: 2278-7461, p-ISSN: 2319-6491
Volume 13, Issue 12 [December. 2024] PP: 161-168

A Machine Vision-Based Method for Detecting Side Wear of End Mills

Yueqian Hou[1],Yuanlong Bai[1],Zhengyi Hu[2],Chengyang Deng[1]
[1] *Shool of Mechanical and Vehicle Engineering, Changchun University, Changchun, CHINA*
[2] *Scientific Research Department, Changchun technical university of Automobile, Changchun, CHINA*
Corresponding Author: Yueqian Hou

ABSTRACT: *In response to the limitations of traditional machine vision methods, which often neglect wear on other side edges and fail to effectively process the worn regions, this paper proposes a machine vision-based method for detecting side wear on end mills, aiming to improve measurement accuracy. The side edge region of the end mill is extracted through local threshold segmentation and the minimum enclosing rectangle method, enabling the regional processing of end mill images. Using the extracted side edge images, the Sobel algorithm is employed to effectively identify the wear edges. Polynomial fitting is then applied to reconstruct the ideal edge of the side blade, and the wear width is subsequently calculated. In the experiments, a three-fluted end mill with a diameter of 16mm is selected as the test object to measure the wear on its side edges. The experimental results show that the goodness of fit for the reconstructed side edge of the end mill approaches 1, with the standard error significantly lower than that of traditional methods. The average measurement accuracy for wear detection reaches 94.68%, demonstrating the high precision and stability of this method in end mill wear detection.*
Key words: *Machine vision; End mill wear; Edge detection; Image processing*

Date of Submission: 14-12-2024 Date of acceptance: 28-12-2024

I. INTRODUCTION

In high-end manufacturing milling processes, tool wear directly impacts machining quality. Changes in tool condition significantly affect the precision and surface quality of the final product [1]. Excessive tool wear not only degrades the quality of the machined surface but is also one of the primary causes of unexpected downtime [2]. Statistics indicate that tool-related expenses, including replacement costs, account for approximately 25% of total costs, while tool failures contribute to 35% of total milling machine downtime [3]. Additionally, downtime caused by tool replacement constitutes 20% of overall downtime [4]. To mitigate the adverse effects of tool wear on machining, tools must be replaced before they fail. However, traditional manual inspection is heavily influenced by subjective judgment. Replacing tools before they reach the wear threshold results in wasted resources, whereas continuing to use severely worn tools may lead to safety incidents. Therefore, a tool wear detection method is needed to enhance tool utilization, improve the machined surface quality, and reduce safety risks.

Tool wear measurement can generally be divided into direct and indirect methods. Indirect measurement methods assess tool wear by monitoring changes in cutting force, machine power, vibration, and acoustic emission signals during machining [5]. Móricz L. et al. [6] utilized spindle power signals and artificial neural networks to achieve both offline and online monitoring of micro-tool wear in ceramic machining, establishing the relationship between wear stages and measured parameters. Similarly, Zhou et al. [7] developed a wireless rotary vibration measurement tool holder system capable of simultaneously measuring vibration signals across three axes. However, indirect measurement methods typically rely on expensive specialized experimental equipment, and the results are often susceptible to external factors and experimental conditions. Since these methods infer tool wear by analyzing signal variations, they face challenges in accurately reflecting actual wear values, and their measurement precision is often lower than that of direct measurement methods.

To optimize the accuracy of tool wear detection, direct measurement methods typically employ optical sensors to monitor tool wear in real-time during the machining process. These sensors can detect changes in the tool's appearance, surface features, and geometric shape. Yu et al. [8] proposed a machine vision method based on local image features for monitoring tool wear. This method first removes background noise from the tool image using a non-local means filter, then enhances the wear region using adaptive contrast, and finally detects local extrema of the wear region boundaries through morphological reconstruction, effectively extracting the wear boundaries. Furthermore, Zhichao You et al. [9] introduced the concept of a Tool Condition Image Sequence (TCIS), which measures tool wear characteristics from multiple angles and integrates the data from each angle to accurately assess wear on the tool's side wings.

Existing machine vision methods typically focus on analyzing the wear regions near the bottom edge of the end mill, neglecting wear on other parts of the side edges during the milling process. Traditional wear region fitting measurements often concentrate on local analysis and simplify the tool edge to a straight line. However, since wear on the side edges of the end mill may be uniformly distributed and the overall wear in this region is relatively smooth, local analysis fails to effectively capture the fluctuations in these areas, leading to incorrect wear position identification and, consequently, reduced measurement accuracy. To address this issue, this paper proposes a regional processing strategy and optimizes the edge reconstruction algorithm for the wear region, significantly improving measurement accuracy.

II. Tool Wear Detection System Design

To address the issue that existing machine vision methods struggle to accurately capture wear images of the side edges of end mills, which impacts measurement accuracy, this paper presents a tool wear detection system as shown in Figure 1. The system primarily consists of a CMOS camera, lens, dome light source, and three-jaw chuck. The CMOS camera provides high-definition images, ensuring that tool details are captured with precision. The dome light source is ideal for high-reflective surfaces, offering uniform illumination that effectively minimizes reflection interference. The three-jaw chuck securely holds the tool, ensuring its positional stability. By fixing the tool to the three-jaw chuck and utilizing the uniform illumination from the dome light source, the wear features of the tool are clearly highlighted. Ultimately, the camera captures images of the tool's side edge, completing the image acquisition process.

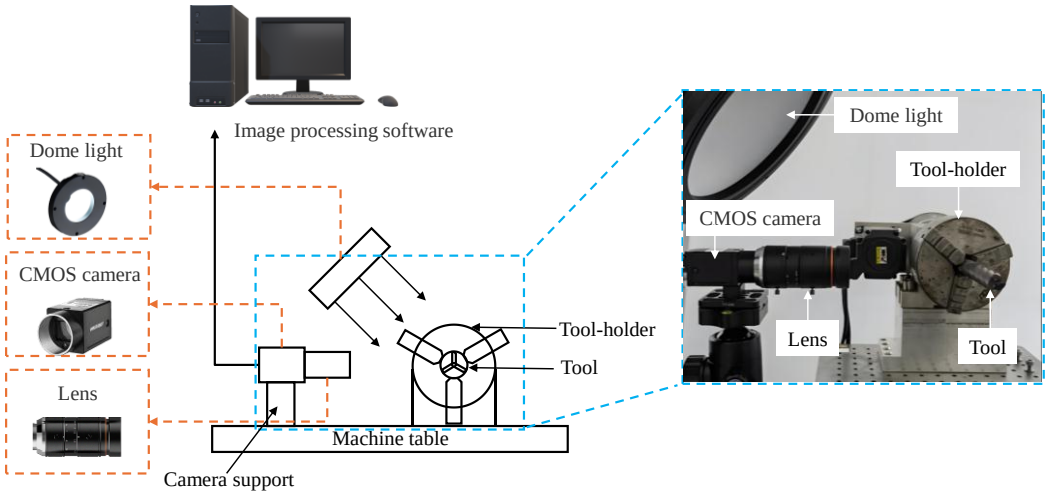

Fig. 1 Schematic diagram of tool wear monitoring platform

III. Side Edge Position Extraction

The data source is affected by issues such as noise, uneven lighting, and blurry edges, which significantly impact the measurement of wear on the side edges of end mills. Therefore, image preprocessing is essential to improve image quality and enhance the features of the regions of interest, thereby improving the accuracy of wear measurements. When denoising and enhancing the entire image, processing time is prolonged, and irrelevant edge information may cause interference, increasing the difficulty of subsequent wear measurements. An analysis of end mill images reveals that the tool body and background occupy most of the image, while the side edge region, which is critical for wear measurement, occupies less than one-tenth of the total area. To address this, this paper proposes a regional processing strategy, using local threshold segmentation to detect the side edge region of the end mill. The position information of the side edge is then obtained using the minimum enclosing rectangle method, and the region is cropped from the original image for separate processing. The specific workflow is shown in Figure 2. This method avoids unnecessary image processing steps, thereby improving the accuracy of side edge wear measurements.

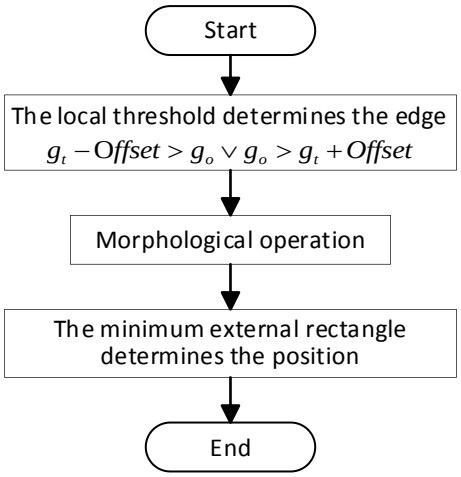

Fig. 2 End Mill Side Edge Extraction Process

Local Threshold Segmentation Method

When analyzing the acquired images, the background grayscale is often complex, and a single threshold is insufficient to effectively extract the required grayscale information. In this context, selecting an appropriate thresholding algorithm is crucial. Compared to fixed thresholding methods, local thresholding is more suitable for extracting edge information where there are significant amplitude changes in the foreground signals. The key to local thresholding is constructing a threshold matrix that adapts to the local features of the image. The specific steps of this method include: first, reading the image; then, performing mean filtering to smooth the original image; and finally, comparing the smoothed image with the local pixels of the original image to extract regions where the pixel differences exceed a set threshold.

First, select an n * n pixel neighborhood in the image as a fixed window and calculate the average pixel value within this window to reduce local grayscale fluctuations. Then, set an offset as a threshold to adjust the local average value. In the local region, compare the grayscale value (g_0) of each pixel with the smoothed average grayscale value (g_t) of the surrounding area. If the pixel value in the original image is smaller than the smoothed image pixel value minus the offset, or greater than the smoothed image pixel value plus the offset, the point is selected.

$$g_t - Offset > g_o \vee g_o > g_t + Offset \quad (1)$$

Where: $offset$ is the offset, g_0 is the grayscale value in the original image, and g_t is the average grayscale value in the neighborhood region.

End Mill Side Edge Region Extraction

To extract a continuous target region and reduce interference, local threshold segmentation is first applied. However, the segmentation results often include short, scattered lines, leading to a lack of coherence in the region. To enhance the integrity of the target region, morphological operations, such as filling gaps and closing operations, are combined to effectively remove irrelevant parts. Through these steps, the coherence of the target region is strengthened, and the different side edges are successfully separated into independent regions, facilitating the subsequent identification of each side edge's location and cropping.

After completing the initial region segmentation, pixel-level edge detection is used to quickly locate the side edges. However, the pixel-level detection results may introduce errors. To ensure the side edges are fully included in the cropped region, dilation is applied to the detected edge, using a circular structuring element with a radius of R to expand the recognition range, thereby extracting the complete side edge image. Subsequently, the minimum enclosing rectangle method is employed. By extracting the extreme horizontal and vertical coordinates of the high pixel value points, information such as the center coordinates, dimensions, and rotation angle of the smallest rectangle is determined. Finally, based on the positioning information of the minimum enclosing rectangle, the corresponding region is cropped from the original image, ensuring the completeness and accuracy of the area coverage for subsequent analysis and wear measurement. The cropping result is shown in Figure 3.

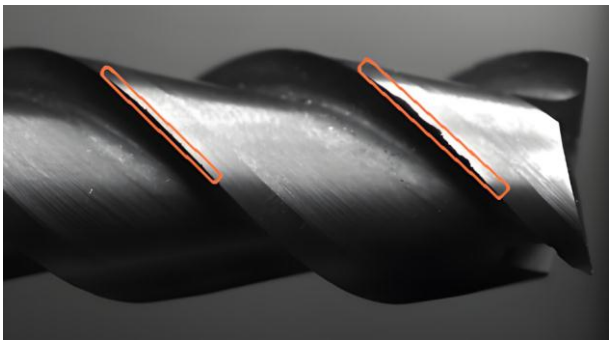

Fig. 3 End Mill Side Edge Cropping Result Image

IV. Side Edge Position Extraction

To measure the wear value, it is necessary to reconstruct the worn spiral cutting edge to obtain the ideal spiral cutting edge. This paper uses a polynomial fitting method to reconstruct the ideal edge of the end mill side edge. This method more accurately describes the non-linear variation of the worn edge, avoiding interference from local errors and improving the overall reconstruction accuracy. The edge curve is then fitted using the least squares method to complete the wear edge reconstruction of the entire side edge.

Image Preprocessing

The side edge region extracted from the original image often suffers from issues such as low contrast, blurred edges of the end mill side, and noise, which makes it difficult to accurately detect the side edge. To improve the image quality and enhance the detectability of relevant information, making it more suitable for subsequent image analysis and processing, this paper applies guided filtering and Gamma correction.

In image filtering processes, commonly used methods such as Gaussian filtering, median filtering, and mean filtering can smooth out noise, but they often result in the loss of edge details in the image, as they cannot distinguish between noise and edge details. To address this issue, this paper employs the guided filtering method. Guided filtering directs the filtering process based on the local structure of the image, taking into account the neighborhood relationships of pixels and utilizing the edge information of the guidance image. This approach effectively reduces noise and smooths the image while preserving sharp edges. The calculation is given by Equation 2:

$$q_i = \sum_j W_{ij}(I) \cdot p_j \tag{2}$$

In the equation: The original image being processed is denoted as p, the guidance image is I, and the filtered output is denoted as q. The output image obtained by filtering with a window centered at is represented as q_i, and W_{ij} is the filtering kernel.

To address the issue of image quality degradation caused by uneven lighting distribution, this paper employs the Gamma correction method. By adjusting the brightness balance of the image, this technique effectively enhances the overall image quality. The corresponding formula is as follows:

$$f(I_i) = I_i^{\gamma} \tag{3}$$

In the equation: $f(I_i)$ is the transformed pixel value; I_i is the original pixel value; γ is the adjustable parameter that affects the enhancement effect.

Subpixel Contour Extraction

Using the methods described above, high-quality side edge images of the end mill suitable for edge detection can be obtained. Common edge detection methods include Canny, Sobel, and Roberts. The Canny algorithm uses non-maximum suppression during the detection process, retaining edges with local maximum gradients and effectively removing weaker or discontinuous edges. However, this may lead to some discontinuities in the edge segments. In contrast, the Sobel algorithm is more sensitive to small gradient changes in the image, generating more continuous edge segments, which makes it particularly suitable for detecting smoother edges. Therefore, the Sobel algorithm is used to extract the edge contours, and the result is shown in Figure 4.

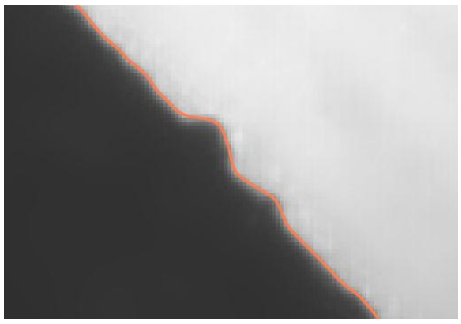

Fig. 4 Subpixel-level Edge Contour Image

Wear Edge Reconstruction

Traditional wear fitting methods typically focus on local analysis and often simplify the tool edge to a straight line. However, this approach has significant limitations when dealing with side edge wear of end mills. Specifically, in cases of uniform and smooth wear, local analysis can easily lead to misjudgment of the wear position, thereby affecting measurement accuracy. To address this issue, this paper adopts a polynomial fitting method that utilizes the entire edge information for fitting, effectively reducing the interference of local wear data in edge reconstruction. Polynomial fitting captures the smooth variations of the worn area more accurately by fitting the overall geometry of the tool edge, thereby enhancing the precision and stability of wear measurements.

After projecting the helical trajectory of the milling cutter onto a two-dimensional plane, the trajectory can be divided into multiple curve segments. By using the least squares method for cubic polynomial fitting, the trend of edge variations can be accurately described. Additionally, a quadratic fitting method is employed to reconstruct the ideal curve, which helps generate an edge contour that closely approximates the real edge shape despite noise interference.

Assume that the cubic curve equation for the ideal edge fitting is given by:

$$\hat{y} = ax^3 + bx^2 + cx + d \tag{4}$$

By substituting N data points into equation (4), we obtain the matrix equation:

$$\begin{bmatrix} x_1^3 & x_1^2 & x_1 & 1 \\ x_2^3 & x_2^2 & x_2 & 1 \\ \vdots & \vdots & \vdots & \vdots \\ x_N^3 & x_N^2 & x_N & 1 \end{bmatrix} \begin{bmatrix} a \\ b \\ c \\ d \end{bmatrix} = \begin{bmatrix} y_1 \\ y_2 \\ \vdots \\ y_N \end{bmatrix} \tag{5}$$

The optimal solution for the parameters can be obtained by minimizing the error:

$$X = (A^T A)^{-1} A^T B \tag{6}$$

Here, a, b, c, and d are the coefficients of the cubic fit. x_i and y_i represent the horizontal and vertical coordinates of the subpixel edge points, respectively, and mmm denotes the number of subpixel edge points.

By solving this equation, the fitting coefficients a, b, c, and d can be obtained, thereby reconstructing the ideal edge.

After the worn edge is reconstructed, the original profile fitted with the ideal edge is compared to the worn profile, and the difference between the two is calculated. This allows for an accurate determination of the side cutting edge wear width of the end mill. The fitting results are shown in Figure 5.

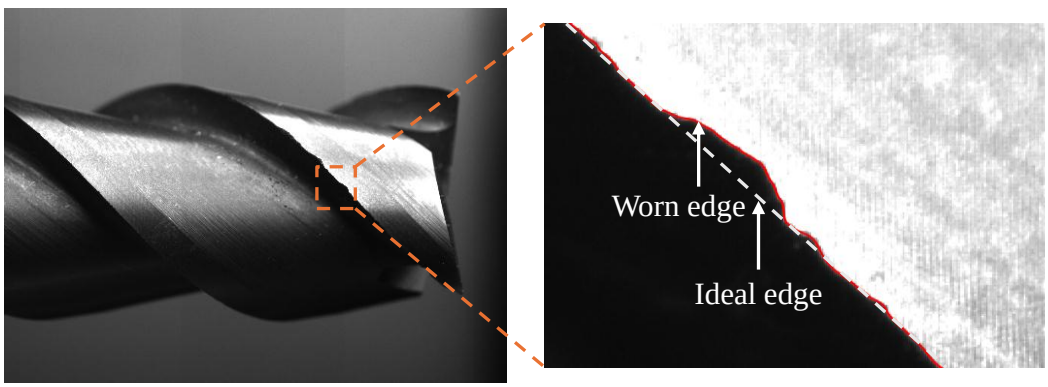

Fig. 5 Reconstructed Image of the Worn Edge

V. Analysis of the Algorithm's Effectiveness

To validate the advantages of the proposed method for flank wear detection in end mills, a three-flute end mill with a diameter of 16 mm and a helix angle of 45° was selected. The wear images of the rear flank of the end mill were captured, and a comparative analysis of the method's performance was conducted. The goodness of fit and standard error were used as evaluation metrics to compare the effectiveness of the traditional linear fitting method and the polynomial fitting method in reconstructing the worn edge. Additionally, a comparison of the pixel distance results for both methods was performed.

Analysis of Goodness of Fit and Standard Error

The goodness of fit is used to measure the quality of the model's fit to the data, with a range from 0 to 1. A value closer to 1 indicates a stronger explanatory power of the model and more accurate reconstruction results [10]. The standard error evaluates the average deviation between the sample points and the predicted values. A smaller value signifies lower error and higher reconstruction accuracy. In the reconstruction of the flank wear edge, the combined use of these two metrics provides a comprehensive evaluation of the model's performance. The goodness of fit primarily characterizes the overall fitting ability of the model, while the standard error further reflects the model's local error level, thus providing a scientific basis for optimizing the edge reconstruction algorithm. The comparison results of different methods are shown in Tables 1 and 2.

Additionally, Figure 6 presents a comparative analysis of the edge reconstruction results for the same wear region of the end mill using different methods. It is clearly visible from the figure that the polynomial fitting method exhibits significant advantages over the linear fitting method in terms of both accuracy and robustness.

Table 1: Comparison of Goodness of Fit Results for Different Methods

Experimental Group	linear fitting method	polynomial fitting method
1	0.994753	0.999794
2	0.998180	0.999145
3	0.995730	0.998267
4	0.991541	0.995813
5	0.997609	0.999889

Table 2: Comparison of Standard Error Results for Different Methods

Experimental Group	linear fitting method	polynomial fitting method
1	12.88800	1.53819
2	6.82745	4.47037
3	2.62007	1.86381
4	4.39458	3.10873
5	8.06302	1.41803

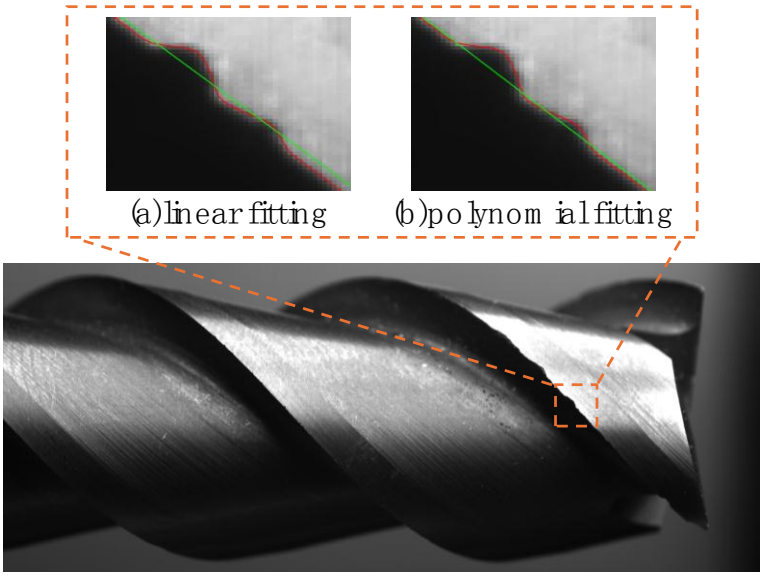

Fig. 6 Comparison of Reconstruction Results

The comparison results indicate that the linear fitting method fails to accurately describe complex, continuous wear regions, especially in larger wear scenarios where significant errors occur. The polynomial-based edge fitting method used in this study, by optimizing the two key metrics—goodness of fit and standard error—not only significantly improves the overall fitting quality of the edge reconstruction, but also effectively reduces errors in local regions, ensuring higher accuracy and stability.

Analysis of Relative Error

By comparing the fitted original profile with the worn profile and calculating the difference between them, the wear width can be accurately determined. The maximum wear pixel value manually identified using image processing software in Table 3 is taken as the true wear pixel value. The measurement error of the proposed algorithm is analyzed through relative error. Let Da denote the true wear pixel value, and the formula for calculating the relative error is:

$$E_{rr} = \frac{|D_a - D_m|}{D_a} \times 100\% \tag{7}$$

Table 3: End Mill Wear Measurement Data

Experimental Group	D_a/pixel	D_m/pixel	Δ/pixel	E_{rr}（%）
1	2.37127	2.32243	0.04884	2.06
2	2.97178	2.80983	0.16195	5.76
3	3.12742	3.03150	0.09592	3.07
4	3.20742	3.08652	0.12090	3.92
5	3.56903	3.34813	0.22090	6.19
6	4.21287	3.97278	0.24009	5.70
7	4.65166	4.37876	0.27290	5.87
8	5.10989	4.83553	0.27436	5.67
9	5.15257	4.77474	0.37783	7.33
10	5.33598	4.95981	0.37617	7.58

The results show that, in the 10 sets of experimental data, the maximum and minimum absolute errors between the measurement values obtained by the vision system and the true values are 0.37783 pixel and 0.04884 pixel, respectively. The maximum and minimum relative errors are 2.06% and 7.58%, respectively. The average

relative deviation (Err) is 5.32%, meaning the average accuracy reaches 94.68%. Based on the above analysis, the detection algorithm of the machine vision system can effectively extract and reconstruct the profile of the end mill's side cutting edge, ensuring high detection accuracy and system stability. This algorithm not only demonstrates excellent precision but also exhibits strong robustness and adaptability.

VI. CONCLUSION

This paper presents a machine vision-based method for end mill wear detection, utilizing a local thresholding technique to identify the side cutting edge region, and applying guided filtering and gamma correction algorithms for image denoising and enhancement. The local thresholding-based region processing strategy avoids redundant image processing, improving measurement accuracy. The polynomial edge fitting method demonstrates strong fitting capability and precision, with a goodness of fit close to 1 and a standard error significantly lower than that of traditional methods, effectively addressing the issue of complex edge reconstruction. Experimental results show that the maximum absolute error of the proposed method across 10 sets of experimental data does not exceed 0.4 pixel, and the average accuracy reaches 94.68%. The extracted wear profile aligns with the actual one, meeting the practical requirements of tool wear detection in industrial settings. This method exhibits high accuracy and reliability for industrial applications in tool wear detection.

Acknowledgements

We acknowledge the support from the the Jilin Provincial Department of Education (Grant JJKH20241757CY).

REFRENCES

[1]. Qiang L, Ya-Dong G, Ming C, et al. Research on surface integrity in milling Inconel718 superalloy[J]. International journal of advanced manufacturing technology, 2017, 92(1-4): 1449-1463.

[2]. Javed K, Gouriveau R, Li X, et al. Tool wear monitoring and prognostics challenges: a comparison of connectionist methods toward an adaptive ensemble model[J]. Journal of Intelligent Manufacturing, 2018, 29(8): 1873-1890.

[3]. Liu C, Wang G F, Li Z M. Incremental learning for online tool condition monitoring using Ellipsoid ARTMAP network model[J]. Applied soft computing, 2015, 35: 186-198.

[4]. Vetrichelvan G, Sundaram S, Senthil Kumaran S, et al. An investigation of tool wear using acoustic emission and genetic algorithm[J]. Journal of vibration and control, 2015, 21(15): 3061-3066.

[5]. Malekian M, Park S S, Jun M B G. Tool wear monitoring of micro-milling operations[J]. Journal of materials processing technology, 2009, 209(10): 4903-4914.

[6]. Móricz L, Viharos Z J, Németh A, et al. Off-line geometrical and microscopic & on-line vibration based cutting tool wear analysis for micro-milling of ceramics[J]. Measurement : journal of the International Measurement Confederation, 2020, 163: 108025.

[7]. Zhou C A, Guo K, Zhao Y, et al. Development and testing of a wireless rotating triaxial vibration measuring tool holder system for milling process[J]. Measurement : journal of the International Measurement Confederation, 2020, 163: 108034.

[8]. Yu J, Cheng X, Zhao Z. A machine vision method for measurement of drill tool wear[J]. International journal of advanced manufacturing technology, 2022, 118(9-10): 3303-3314.

[9]. You Z, Gao H, Guo L, et al. Machine vision based adaptive online condition monitoring for milling cutter under spindle rotation[J]. Mechanical systems and signal processing, 2022, 171: 108904.

[10]. Kamasak M E, Christian B T, Bouman C A, et al. Quality and Precision of Parametric Images Created From PET Sinogram Data by Direct Reconstruction: Proof of Concept [J]. IEEE Transactions on Medical Imaging, 2014, 33(3): 695-707.